

## Supporting Information

# A Lithium-Scandium Sulfate with Second-Harmonic Generation Response and Deep-Ultraviolet Transparency

Zi-Long Geng,<sup>a,c</sup> Hong-Xin Tang,<sup>a</sup> Rui-Biao Fu,<sup>\*,a</sup> Zu-Ju Ma,<sup>\*,b</sup> and Xin-Tao Wu<sup>a</sup>

a. State Key Laboratory of Structural Chemistry, Fujian Institute of Research on the Structure of Matter, Chinese Academy of Sciences, Fuzhou, Fujian 350002, China.

b. School of Environmental and Materials Engineering, Yantai University, Yantai, Shandong 264005, China.

c. University of Chinese Academy of Sciences, Beijing 100049, China.

\* E-mail addresses: furb@fjirsm.ac.cn (R.-B. Fu), zjma@outlook.com (Z.-J. Ma)

# Contents

Synthesis .....	2
Single-Crystal X-ray Diffraction .....	2
Powder X-ray Diffraction .....	2
Energy Dispersive X-ray Spectroscopic and Elemental Analyses. ....	2
IR Spectroscopy.....	2
UV-Vis-NIR Diffuse Reflectance Spectroscopy. ....	3
SHG Test.....	3
LDT Measurement.....	3
Computational Details. ....	3
<b>Table S1.</b> Crystal data and structure refinements for <b>Li(H<sub>2</sub>O)<sub>2</sub>Sc(SO<sub>4</sub>)<sub>2</sub></b> . ....	5
<b>Table S2.</b> Atomic coordinates, equivalent isotropic displacement parameters (Å <sup>2</sup> ) and BVS of <b>Li(H<sub>2</sub>O)<sub>2</sub>Sc(SO<sub>4</sub>)<sub>2</sub></b> .....	6
<b>Table S3.</b> Anisotropic displacement parameters (Å <sup>2</sup> ) of <b>Li(H<sub>2</sub>O)<sub>2</sub>Sc(SO<sub>4</sub>)<sub>2</sub></b> . ....	6
<b>Table S4.</b> Selected bond lengths (Å) and angles (deg.) for <b>Li(H<sub>2</sub>O)<sub>2</sub>Sc(SO<sub>4</sub>)<sub>2</sub></b> . ....	7
<b>Table S5.</b> Selected hydrogen bond lengths (Å) and angles (deg.) .....	7
<b>Figure S1.</b> A photograph of the as-grown crystal without polishing for <b>Li(H<sub>2</sub>O)<sub>2</sub>Sc(SO<sub>4</sub>)<sub>2</sub></b> .. ....	8
<b>Figure S2.</b> Experimental and simulated PXRD patterns of <b>Li(H<sub>2</sub>O)<sub>2</sub>Sc(SO<sub>4</sub>)<sub>2</sub></b> . ....	8
<b>Figure S3.</b> EDS spectrum of <b>Li(H<sub>2</sub>O)<sub>2</sub>Sc(SO<sub>4</sub>)<sub>2</sub></b> . ....	9
<b>Figure S4.</b> IR spectrum of <b>Li(H<sub>2</sub>O)<sub>2</sub>Sc(SO<sub>4</sub>)<sub>2</sub></b> . ....	9
<b>Figure S5.</b> -COHP and partial density of state (PDOS) for (a) Li-O9 and (b) Li-O10 bonds. ....	10
<b>Figure S6.</b> The coordination environments of S1(VI) and S2(VI) atoms.....	11
<b>Figure S7.</b> -COHP and PDOS for (a) Li-O4 and (b) Li-O8 bonds. ....	11
<b>Figure S8.</b> UV-Vis-NIR spectrum of <b>Li(H<sub>2</sub>O)<sub>2</sub>Sc(SO<sub>4</sub>)<sub>2</sub></b> . ....	12
<b>Figure S9.</b> The calculated band structure of <b>Li(H<sub>2</sub>O)<sub>2</sub>Sc(SO<sub>4</sub>)<sub>2</sub></b> . ....	12
<b>Figure S10.</b> Optical refractive indices along principal axes birefringence Δn.....	13
<b>Figure S11.</b> Frequency-dependent SHG coefficient  d <sub>36</sub>   of <b>Li(H<sub>2</sub>O)<sub>2</sub>Sc(SO<sub>4</sub>)<sub>2</sub></b> .....	13
<b>Figure S12.</b> PDOS of oxygen in water molecules and [SO <sub>4</sub> ] groups in <b>Li(H<sub>2</sub>O)<sub>2</sub>Sc(SO<sub>4</sub>)<sub>2</sub></b> .....	14
References.....	15

## Synthesis

Lithium nitrate ( $\text{LiNO}_3$ , 99.0%) was purchased from Shanghai Macklin Biochemical Co., Ltd. Scandium oxide ( $\text{Sc}_2\text{O}_3$ , 99.9%+) was purchased Shanghai Titan Scientific Co., Ltd. Sulfuric acid ( $\text{H}_2\text{SO}_4$ , 95.0%~98.0%) was obtained from Sinopharm Reagent and used as received.

**The synthesis of  $\text{Li}(\text{H}_2\text{O})_2\text{Sc}(\text{SO}_4)_2$ :** A mixture of  $\text{LiNO}_3$  (275.8 mg, 4.0 mmol),  $\text{Sc}_2\text{O}_3$  (110.3 mg, 0.8 mmol),  $\text{H}_2\text{SO}_4$  (0.2 mL) and distilled water (1 mL) was added into the Teflon-lined stainless-steel autoclaves. The whole reactor was placed in a muffle furnace, heated from room temperature to 235 °C for 120 min, and held at 235 °C for 4 days, and then gradually cooled to 30 °C at a rate of 4 °C·h<sup>-1</sup>. The product was filtered and washed with anhydrous ethanol. A large amount of  $\text{Li}(\text{H}_2\text{O})_2\text{Sc}(\text{SO}_4)_2$  colorless crystal was obtained (Fig. S1). Its yield based on  $\text{Sc}_2\text{O}_3$  yield is more than 90%. Experimental PXRD patterns accord well with those simulated from single-crystal X-ray diffraction data, that proves its phase purity (Fig. S2).

## Single-Crystal X-ray Diffraction

Single-crystal X-ray diffraction data of  $\text{Li}(\text{H}_2\text{O})_2\text{Sc}(\text{SO}_4)_2$  was collected by using graphite-monochromated Ga K $\alpha$  radiation ( $\lambda(\text{Ga-K}\alpha) = 1.3405 \text{ \AA}$ ) with a Rigaku Oxford Diffraction. Data reduction was integrated with the program Crystal Clear version 1.30. The structure was solved with a direct method using the SHELXT and refined by the SHELXL full-matrix least-squares program.<sup>1-2</sup> The structure was checked by the PLATON<sup>3</sup> and no higher symmetries were suggested. Details of crystallographic data are listed in Table S1. Atomic coordinates, equivalent isotropic displacement parameters and bond valence sum (BVS) for  $\text{Li}(\text{H}_2\text{O})_2\text{Sc}(\text{SO}_4)_2$  are summarized in Tables S2-S4, respectively. CCDC 2242833 for  $\text{Li}(\text{H}_2\text{O})_2\text{Sc}(\text{SO}_4)_2$ .

## Powder X-ray Diffraction

Powder XRD pattern was collected at room temperature using a Rigaku Miniflex 600 diffractometer with Cu K $\alpha$  radiation ( $\lambda = 1.540598 \text{ \AA}$ ). Powder XRD data was obtained in the 2 $\theta$  range of 5-55° with a step width of 0.02° (Fig. S2).

## Energy Dispersive X-ray Spectroscopic and Elemental Analyses

Elemental analyses were performed by using a field emission scanning electron microscope (FESEM, JSM6700F) with an energy dispersive X-ray spectroscope (EDS, Oxford INCA). The result verifies that the product contains Sc, O and S elements (Fig. S3). Furthermore, the atomic ratio of Sc:S:O is 1:1.95:9.16 which is in good agreement of the theoretical value of 1:2:10. Elemental analyses H was carried out with a Vario EL III element analyzer. Anal. Calcd. for  $\text{Li}(\text{H}_2\text{O})_2\text{Sc}(\text{SO}_4)_2$ : H 1.43 %. Found: H 1.55%.

## IR Spectroscopy

IR spectrum was recorded at room temperature on a VERTEX70 FT-IR spectrometer instrument by using Attenuated Total Reflectance (ATR) method. The sample was tightly fitted to the total reflection crystal (**Fig. S4**). Data were collected from 4000 to 400  $\text{cm}^{-1}$ .

## UV-Vis-NIR Diffuse Reflectance Spectroscopy

UV-Vis-NIR diffuse reflectance spectrum was recorded at room temperature on a PrkinElmer Lambda 950 spectrophotometer using  $\text{BaSO}_4$  as the standard reference within the spectral range of 200-2500 nm (**Fig. S8**). The reflection spectrum was calculated into the absorption spectrum by using the Kubelka-Munk function.<sup>4,5</sup> And UV-Vis-NIR ultraviolet transmittance spectrum was recorded at room temperature on a PrkinElmer Lambda 950 spectrophotometer. The measured spectral range is 190-500 nm.

## SHG Test

Powder SHG measurement was performed on a pulsed Q-switched Nd: YAG solid-state laser using the Kurtz-Perry method with a wavelength of 1064 nm at room temperature.<sup>6</sup> Crystalline samples and microcrystalline KDP as the references were ground and sieved into progressively increasing particle size ranges: 25-45, 45-53, 53-75, 75-109, 109-150, 150-212 and 212-270  $\mu\text{m}$ .

## LDT Measurement

LDT measurement was tested on sieved sample of  $\text{Li}(\text{H}_2\text{O})_2\text{Sc}(\text{SO}_4)_2$  with the particle-size range of 212-270  $\mu\text{m}$ , under a 1064 nm laser source (10 ns, 1 Hz and 0.02  $\text{cm}^2$  for laser spot area). The energy of the laser emission was gradually increased until the color of the sample changed.

## Computational Details

Our DFT calculations have been performed using the Vienna *ab initio* simulation package (VASP)<sup>7-9</sup> with the Perdew-Burke-Ernzerhof (PBE)<sup>10</sup> exchange-correlation functional for nonlinear optical calculations and HSE06 functional for electronic structure and linear optical calculations. The projected augmented wave (PAW)<sup>11</sup> potentials have been used to treat the ion-electron interactions. A  $\Gamma$ -centered  $7 \times 7 \times 3$  Monkhorst-Pack grid for the Brillouin zone sampling<sup>12</sup> and a cutoff energy of 500 eV for the plane wave expansion were found to get convergent lattice parameters and self-consistent energies. The structure displayed in this work was visualized by Device Studio<sup>13</sup> and VESTA<sup>14</sup>.

In the calculation of the static  $\chi^{(2)}$  coefficients, the so-called length-gauge formalism derived by Aversa and Sipe<sup>15</sup> and modified by Rashkeev *et al.*<sup>16</sup> is adopted, which has been proved to be successful in calculating the second-order susceptibility for semiconductors and insulators.<sup>17-20</sup> The dynamic SHG coefficient is calculated by the formula developed by Aversa, Sipe and Rashkeev *et al.*<sup>15, 16</sup> In the static case, the imaginary part of the static second-order optical susceptibility can be expressed as:

$$\begin{aligned} & \chi^{abc} \\ &= \frac{e^3}{\hbar^2 \Omega} \sum_{nml,k} \frac{r_{nm}^a (r_{ml}^b r_{ln}^c + r_{ml}^c r_{ln}^b)}{2\omega_{nm} \omega_{ml} \omega_{ln}} [\omega_n f_{ml} + \omega_m f_{ln} + \omega_l f_{nm}] \\ &+ \frac{ie^3}{4\hbar^2 \Omega} \sum_{nm,k} \frac{f_{nm}}{\omega_{mn}^2} [r_{nm}^a (r_{mn;c}^b + r_{mn;b}^c) + r_{nm}^b (r_{mn;c}^a + r_{mn;a}^c) + r_{nm}^c (r_{mn;b}^a + r_{mn;a}^b)] \end{aligned} \quad (1)$$

where  $r$  is the position operator,  $\hbar\omega_{nm} = \hbar\omega_n - \hbar\omega_m$  is the energy difference for the bands  $m$  and  $n$ ,  $f_{mn} = f_m - f_n$  is the difference of the Fermi distribution functions, subscripts  $a$ ,  $b$ , and  $c$  are Cartesian indices, and  $r_{mn;a}^b$  is the so-called generalized derivative of the coordinate operator in  $k$  space,

$$r_{nm;a}^b = \frac{r_{nm}^a \Delta_{mn}^b + r_{nm}^b \Delta_{mn}^a}{\omega_{nm}} + \frac{i}{\omega_{nm}} \times \sum_l (\omega_{lm} r_{nl}^a r_{lm}^b - \omega_{nl} r_{nl}^b r_{lm}^a) \quad (2)$$

where  $\Delta_{nm}^a = (p_{nn}^a - p_{mm}^a) / m$  is the difference between the electronic velocities at the bands  $n$  and  $m$ .

The  $\chi^{(2)}$  coefficients here were calculated from PBE wavefunctions with a  $7 \times 7 \times 3$  k-point grid and about 384 bands. A scissor operator has been added to correct the conduction band energy (corrected to the experimental gap), which has been proved to be reliable in predicting the second-order susceptibility for semiconductors and insulators.<sup>21-23</sup>

**Table S1.** Crystal data and structure refinements for  $\text{Li}(\text{H}_2\text{O})_2\text{Sc}(\text{SO}_4)_2$ .

Empirical formula	$\text{Li}(\text{H}_2\text{O})_2\text{Sc}(\text{SO}_4)_2$
Formula weight	280.05
Temperature(K)	99.99(10)
Crystal color	Colorless
Wavelength(Å)	1.34050
Crystal system	Orthorhombic
Space group	$P2_12_12_1$
<i>a</i> / Å	5.17110(10)
<i>b</i> / Å	8.62070(10)
<i>c</i> / Å	18.5151(2)
Volume / Å <sup>3</sup>	825.38(2)
Z, $\rho_{\text{calcd}}$ / g·cm <sup>-3</sup>	4.2.254
$\mu$ / mm <sup>-1</sup>	8.584
F(000)	560.0
Date / restraints / parameters	1381/6/130
Theta range for data collection	4.152 to 52.019
Limiting indices	$-3 \leq h \leq 6, -10 \leq k \leq 9, -21 \leq l \leq 20$
Reflections collected / unique	1381 [ $R_{\text{int}} = 0.0368, R_{\text{sigma}} = 0.0221$ ]
Completeness	98.7%
Goodness-of-fit on $F^2$	1.100
$R_1, wR_2$ ( $I > 2\sigma$ ) [a]	$R_1=0.0220, R_2=0.0597$
$R_1, wR_2$ (all data)	$R_1=0.0222, R_2=0.0598$
Largest diff ,peak and hole/ e·Å <sup>-3</sup>	0.46 and -0.28
Flack parameter	0.128(19)

[a] $R_1 = \Sigma |F_o| - |F_c| / \Sigma |F_o|$  and  $wR_2 = [\sum w(Fo^2 - Fc^2)^2 / \sum w F_o^4]^{1/2}$ .

**Table S2.** Atomic coordinates, equivalent isotropic displacement parameters ( $\text{\AA}^2$ ) and BVS of  $\text{Li}(\text{H}_2\text{O})_2\text{Sc}(\text{SO}_4)_2$ .

Atom	Wyck.	x	y	z	$U_{\text{eq}}^{\text{a}}$	BVS <sup>b</sup>
Li1	4a	0.4518(12)	0.5526(8)	0.7094(3)	0.0124(13)	1.12
Sc1	4a	0.24034(14)	0.50341(6)	0.47637(3)	0.00640(19)	3.24
S1	4a	0.75063(18)	0.36817(9)	0.58180(4)	0.0069(2)	6.10
S2	4a	0.23117(17)	0.80762(9)	0.59726(4)	0.0069(2)	6.11
O1	4a	0.2295(5)	0.7087(3)	0.53273(12)	0.0106(5)	-2.10
O2	4a	0.4317(5)	0.9282(3)	0.58716(13)	0.0096(6)	-2.03
O3	4a	-0.0221(4)	0.8880(3)	0.60209(14)	0.0084(5)	-1.94
O4	4a	0.2775(5)	0.7220(3)	0.66264(13)	0.0125(5)	-1.92
O5	4a	0.5681(5)	0.4285(3)	0.52747(14)	0.0124(6)	-2.09
O6	4a	1.0161(5)	0.4014(3)	0.55686(14)	0.0106(6)	-2.02
O7	4a	0.7196(5)	0.1981(3)	0.58659(12)	0.0101(5)	-2.00
O8	4a	0.7045(5)	0.4380(3)	0.65158(13)	0.0108(5)	-1.89
O9	4a	0.6713(5)	0.6230(3)	0.78576(15)	0.0151(6)	
O10	4a	0.1631(5)	0.4249(3)	0.74473(14)	0.0135(6)	

<sup>a</sup> $U_{\text{eq}}$  is defined as 1/3 of the trace of the orthogonalised  $U_{ij}$  tensor.

<sup>b</sup>Bond valence sums were calculated by the equation:  $s = \exp [(R_0 - R_i)/b]$ , where  $R_0$  and  $b$  are the bond valence parameters and  $R_i$  is the observed bond lengths.

**Table S3.** Anisotropic displacement parameters ( $\text{\AA}^2$ ) of  $\text{Li}(\text{H}_2\text{O})_2\text{Sc}(\text{SO}_4)_2$

Atom	$U_{11}$	$U_{22}$	$U_{33}$	$U_{23}$	$U_{13}$	$U_{12}$
Li1	0.008(3)	0.011(3)	0.019(3)	0.001(3)	0.003(2)	0.001(3)
Sc1	0.0048(3)	0.0046(3)	0.0098(3)	0.0001(2)	0.0000(3)	0.0002(3)
S1	0.0055(4)	0.0051(4)	0.0100(4)	0.0005(3)	0.0005(4)	0.0000(4)
S2	0.0056(4)	0.0052(4)	0.0099(4)	-0.0001(3)	0.0001(4)	0.0001(3)
O1	0.0065(12)	0.0098(11)	0.0155(12)	-0.0036(9)	0.0015(12)	-0.0009(12)
O2	0.0065(13)	0.0082(13)	0.0140(13)	-0.0015(10)	0.0025(10)	-0.0008(10)
O3	0.0039(12)	0.0079(12)	0.0135(12)	-0.0010(11)	0.0007(10)	0.0013(10)
O4	0.0105(12)	0.0126(12)	0.0146(12)	0.0045(9)	0.0013(11)	0.0021(12)
O5	0.0086(13)	0.0115(14)	0.0169(13)	0.0026(12)	-0.0019(11)	0.0007(10)
O6	0.0067(13)	0.0102(13)	0.0148(13)	0.0011(11)	0.0003(10)	-0.0014(10)
O7	0.0088(12)	0.0061(11)	0.0154(12)	0.0001(9)	-0.0009(11)	0.0001(11)
O8	0.0105(14)	0.0081(11)	0.0138(12)	-0.0019(9)	0.0006(10)	-0.0006(11)
O9	0.0190(15)	0.0108(12)	0.0155(13)	0.0007(11)	0.0018(11)	-0.0013(11)
O10	0.0107(13)	0.0133(12)	0.0166(13)	0.0015(11)	-0.0004(10)	0.0017(10)

**Table S4.** Selected bond lengths ( $\text{\AA}$ ) and angles (deg.) for  $\text{Li}(\text{H}_2\text{O})_2\text{Sc}(\text{SO}_4)_2$ .

Sc(1)-O(1)	2.056(2)	Sc(1)-O(5)	2.046(3)
Sc(1)-O(2) <sup>#1</sup>	2.069(3)	Sc(1)-O(6) <sup>#3</sup>	2.083(3)
Sc(1)-O(3) <sup>#2</sup>	2.121(3)	Sc(1)-O(7) <sup>#4</sup>	2.095(2)
O(1)-Sc(1)-O(2) <sup>#1</sup>	91.27(10)	O(2) <sup>#1</sup> -Sc(1)-O(5)	172.87(11)
O(1)-Sc(1)-O(3) <sup>#2</sup>	89.04(10)	O(3) <sup>#2</sup> -Sc(1)-O(5)	88.63(10)
O(1)-Sc(1)-O(6) <sup>#3</sup>	89.15(10)	O(3) <sup>#2</sup> -Sc(1)-O(6) <sup>#3</sup>	177.56(10)
O(1)-Sc(1)-O(5)	93.42(11)	O(3) <sup>#2</sup> -Sc(1)-O(7) <sup>#3</sup>	90.84(10)
O(1)-Sc(1)-O(7) <sup>#4</sup>	174.39(11)	O(5)-Sc(1)-O(6) <sup>#3</sup>	89.83(11)
O(2) <sup>#1</sup> -Sc(1)-O(3) <sup>#2</sup>	86.08(10)	O(5)-Sc(1)-O(7) <sup>#4</sup>	92.18(10)
O(2) <sup>#1</sup> -Sc(1)-O(6) <sup>#3</sup>	95.61(10)	O(6) <sup>#3</sup> -Sc(1)-O(7) <sup>#4</sup>	91.12(10)
O(2) <sup>#1</sup> -Sc(1)-O(7) <sup>#4</sup>	83.14(10)		

Symmetry transformations used to generate equivalent atoms: #1 -  $1/2 + x, 3/2 - y, 1 - z$ ; #2  $1/2 + x, 3/2 - y, 1 - z$ ; #3 -  $1 + x, y, z$ ; #4 -  $1/2 + x, 1/2 - y, 1 - z$ .

**Table S5.** Selected hydrogen bond lengths ( $\text{\AA}$ ) and angles (deg.) for  $\text{Li}(\text{H}_2\text{O})_2\text{Sc}(\text{SO}_4)_2$ .

D-H $\cdots$ A	D-H	H $\cdots$ A	D $\cdots$ A	angle
O9-H1 $\cdots$ O10 <sup>a</sup>	0.874	1.938	2.797	167.53
O10-H3 $\cdots$ O3 <sup>b</sup>	0.874	2.115	2.945	158.29

Symmetry transformations used to generate equivalent atoms: a: -  $x + 1, y + 1/2, - z + 3/2$ ; b: -  $x, y - 1/2, - z + 3/2$ .

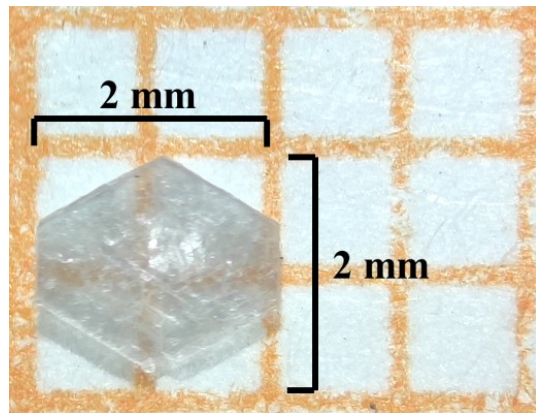


**Figure S1.** A photograph of the as-grown crystal without polishing for  $\text{Li}(\text{H}_2\text{O})_2\text{Sc}(\text{SO}_4)_2$ .

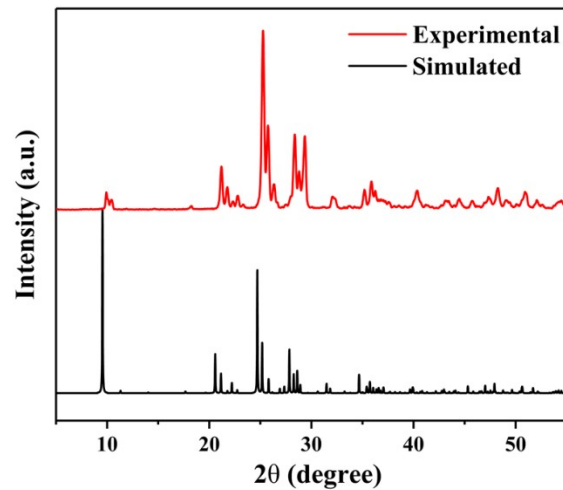


**Figure S2.** Experimental and simulated PXRD patterns of  $\text{Li}(\text{H}_2\text{O})_2\text{Sc}(\text{SO}_4)_2$ .

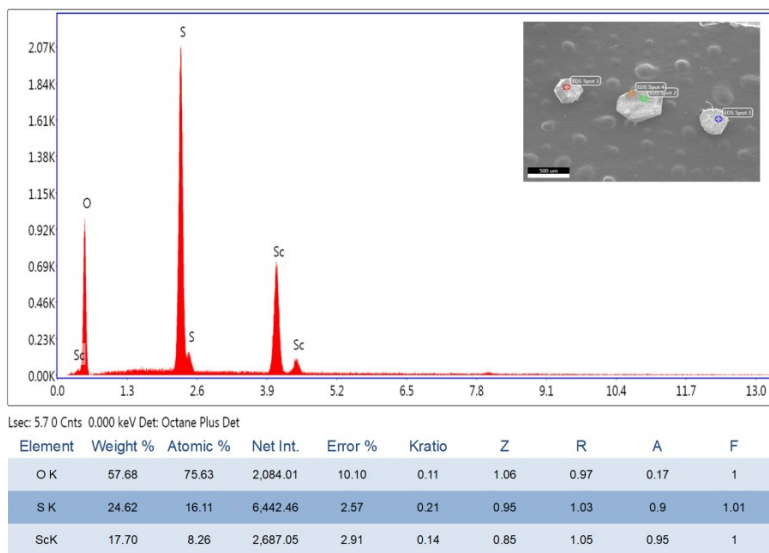


**Figure S3.** EDS spectrum of  $\text{Li}(\text{H}_2\text{O})_2\text{Sc}(\text{SO}_4)_2$ .

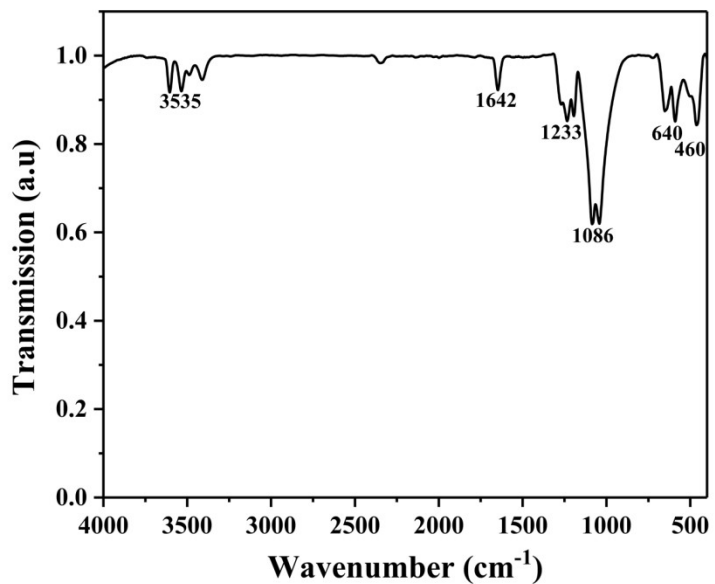
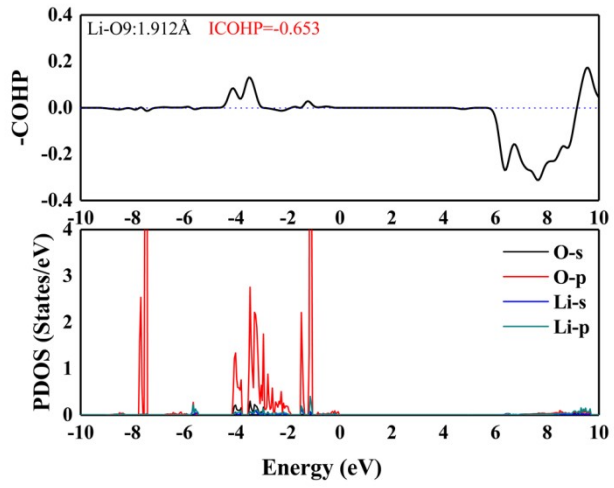
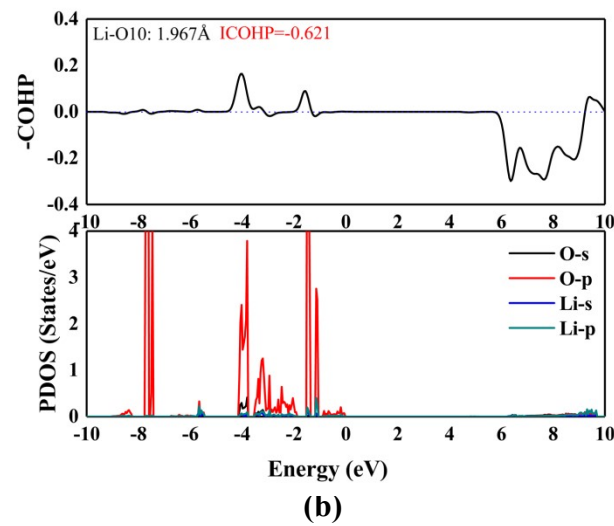


**Figure S4.** IR spectrum of  $\text{Li}(\text{H}_2\text{O})_2\text{Sc}(\text{SO}_4)_2$ .



(a)



(b)

**Figure S5.** -COHP and the partial density of state (PDOS) for (a) Li-O9 and (b) Li-O10 bonds.

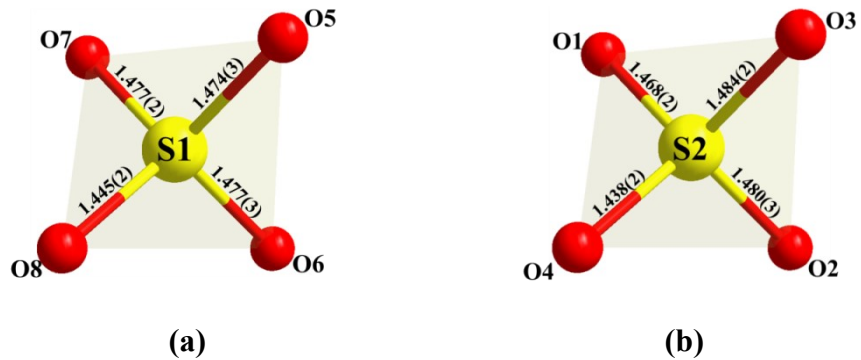


**Figure S6.** The coordination environments of S1(VI) and S2(VI) atoms.

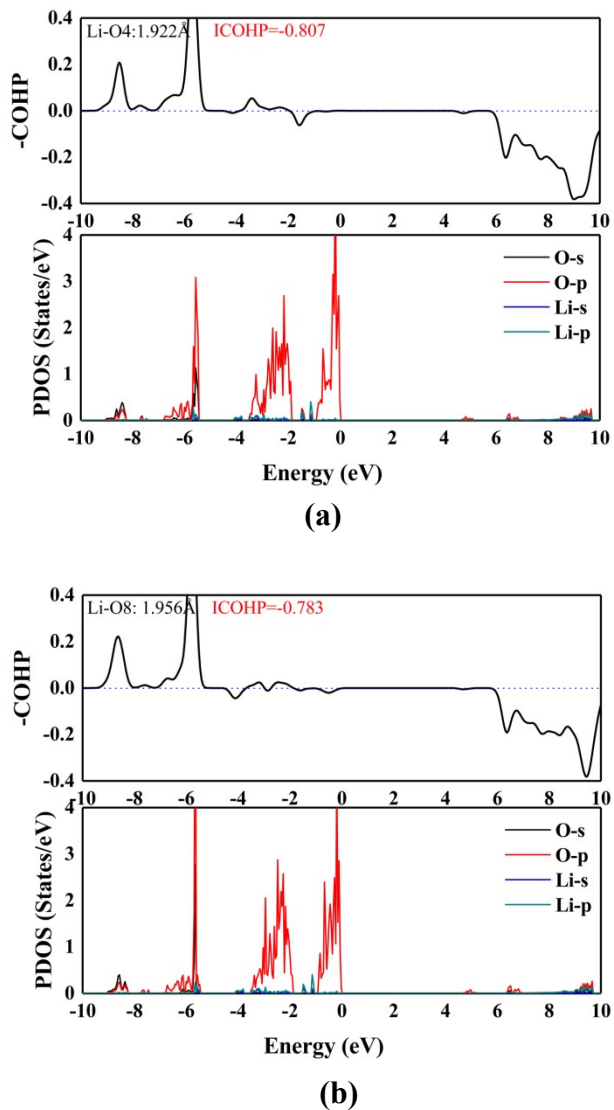


**Figure S7.** -COHP and PDOS for (a) Li-O<sub>4</sub> and (b) Li-O<sub>8</sub> bonds.

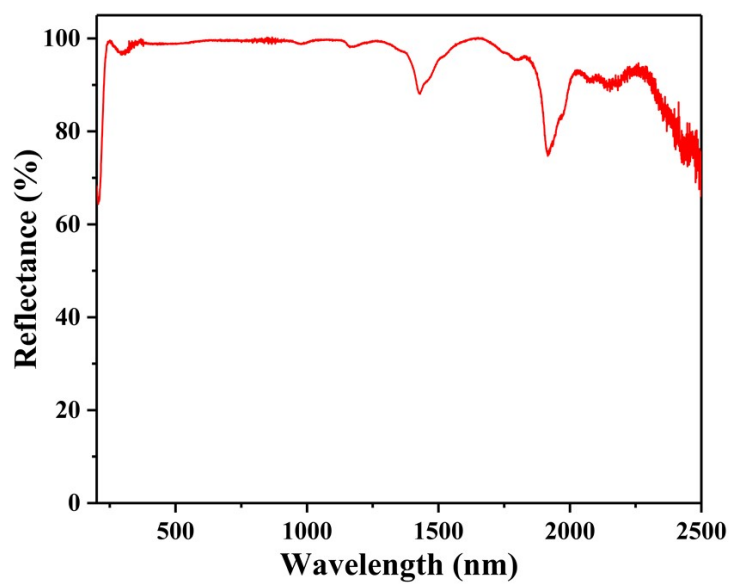


**Figure S8.** The UV-Vis-NIR spectrum of  $\text{Li}(\text{H}_2\text{O})_2\text{Sc}(\text{SO}_4)_2$ .

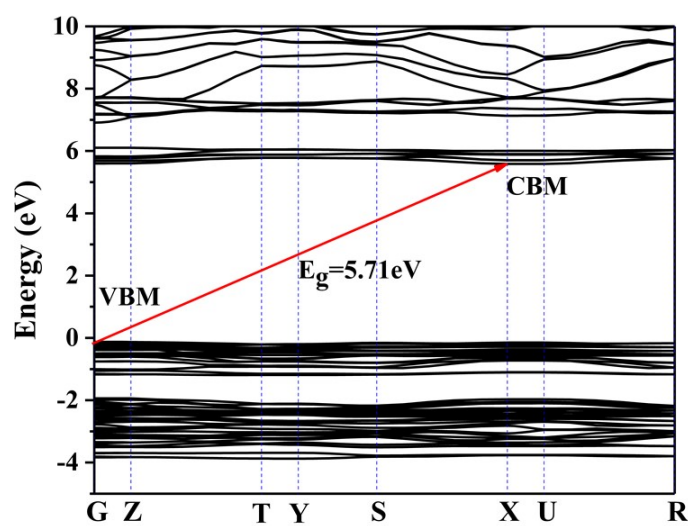


**Figure S9.** The calculated band structure of  $\text{Li}(\text{H}_2\text{O})_2\text{Sc}(\text{SO}_4)_2$ .

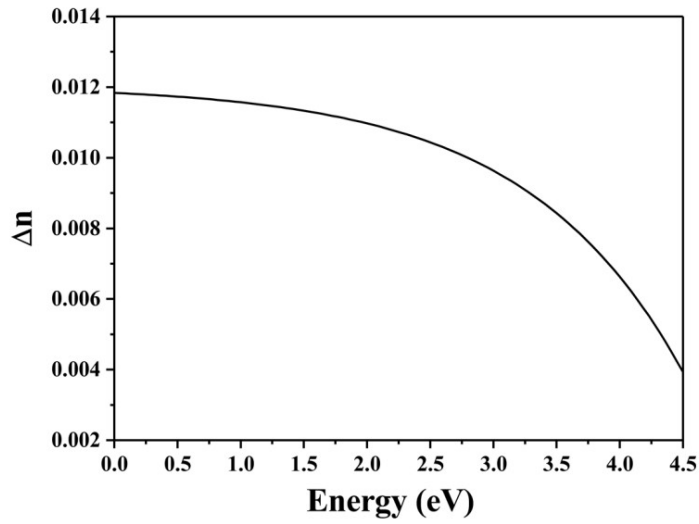


**Figure S10.** The calculated birefringence curve.

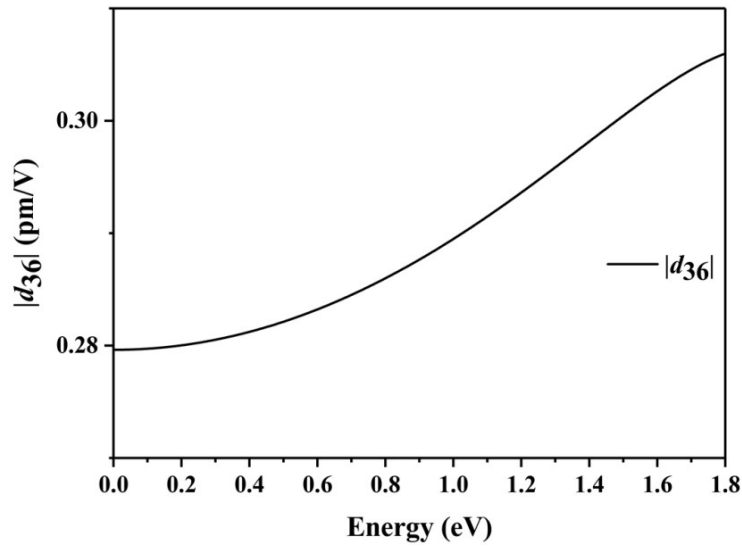


**Figure S11.** The frequency-dependent SHG coefficient  $|d_{36}|$  of  $\text{Li}(\text{H}_2\text{O})_2\text{Sc}(\text{SO}_4)_2$ .

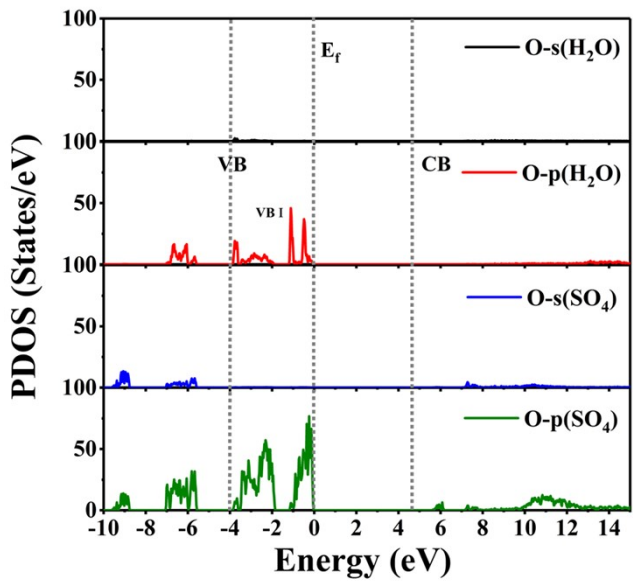


**Figure S12.** PDOS of oxygen in water molecules and [SO<sub>4</sub>] groups in Li(H<sub>2</sub>O)<sub>2</sub>Sc(SO<sub>4</sub>)<sub>2</sub>.

### 3. References

- [1] G. M. Sheldrick, *Acta Cryst.*, 2015, **A71**, 3–8.
- [2] G. M. Sheldrick, *Acta Cryst.*, 2015, **C71**, 3–8.
- [3] A. L. Spek, *J. Appl. Cryst.*, 2003, **36**, 7–13.
- [4] P. Kubelka, F. Z. Munk, *Tech. Phys.*, 1931, **12**, 259-274.
- [5] J. Tauc, *Mater. Res. Bull.*, 1970, **5**, 721-730.
- [6] S. Kurtz, *J. Appl. Phys.*, 1968, **39**, 3798-3813.
- [7] G. Kresse, VASP, 5.3.5; <http://cms.mpi.univie.ac.at/vasp/vasp.html>, 2014.
- [8] G. Kresse, J. Furthmuller, *Phys. Rev. B.*, 1996, **54**, 11169-11186.
- [9] G. Kresse, D. Joubert, *Phys. Rev. B.*, 1999, **59**, 1758-1775.
- [10] J. P. Perdew, K. Burke, M. Ernzerhof, *Phys. Rev. Lett.*, 1996, **77**, 3865-3868.
- [11] P. E. Blochl, *Phys. Rev. B.*, 1994, **50**, 17953-17979.
- [12] H. J. Monkhorst, J. D. Pack, *Phys. Rev. B.*, 1976, **13**, 5188.
- [13] Hongzhiwei Technology, Device Studio, Version 2021A. China, 2021. Available online:<https://iresearch.net.cn/cloudSoftware>.
- [14] K. Momma, F. Izumi, *J Appl. Crystallogr.*, 2011, **44**, 1272-1276.
- [15] C. Aversa, J. E. Sipe, *Phys. Rev. B.*, 1995, **52**, 14636-14645.
- [16] S. N. Rashkeev, W. R. L. Lambrecht, B. Segall, *Phys. Rev. B.*, 1998, **57**, 3905.
- [17] J. Hu, Z. Ma, J. Li, C. He, Q. Li, K. Wu, *J. Phys. D Appl. Phys.*, 2016, **49**, 85103-85103.
- [18] J. Li, Z. Ma, C. He, Q. Li, K. Wu, *J. Mater. Chem. C.*, 2016, **4**, 1926-1934.
- [19] Z. Ma, K. Wu, R. Sa, K. Ding, Q. Li, *Aip Advances*, 2012, **2**, 032170.
- [20] Z. Ma, K. Wu, R. Sa, Q. Li, Y. Zhang, *J. Alloy Compd.*, 2013, **568**, 16-20.
- [21] B. Champagne, D. M. Bishop, *Adv. Chem. Phys.*, 2003, **126**, 41-92.
- [22] A. H. Reshak, S. Auluck, I. V. Kityk, *Phys. Rev. B.*, 2007, **75**, 5120.
- [23] Y. Z. Huang, L. M. Wu, X. T. Wu, L. H. Li, L. Chen, Y. F. Zhang, *J. Am. Chem. Soc.*, 2010, **132**, 12788-12789.